

Acute sensitivity of global ocean circulation and heat content to eddy energy dissipation time-scale

J. Mak^{1,2,3}, D. P. Marshall¹, G. Madec⁴ and J. R. Maddison⁵

¹Department of Physics, University of Oxford

²Department of Ocean Science, Hong Kong University of Science and Technology

³Center for Ocean Research in Hong Kong and Macau, Hong Kong University of Science and Technology

⁴Sorbonne Universités (University Pierre et Marie Curie Paris 6)-CNRS-IRD-MNHN, LOCEAN

Laboratory, Paris

⁵School of Mathematics and Maxwell Institute for Mathematical Sciences, The University of Edinburgh

Key Points:

- Key metrics of global ocean circulation (ACC transport, AMOC strength, OHC anomaly) acutely sensitive to eddy energy dissipation time-scale.
- Modest variations in the dissipation time-scale has an comparable effect to significant variations in the Southern Ocean wind forcing.
- Constraints on the dissipation time-scale critical to long-time integrations of ocean climate models such as paleoclimate scenarios.

arXiv:2204.02074v1 [physics.ao-ph] 5 Apr 2022

Abstract

The global ocean overturning circulation, critically dependent on the global density stratification, plays a central role in regulating climate evolution. While it is well-known that the global stratification profile exhibits a strong dependence to Southern Ocean dynamics and in particular to wind and buoyancy forcing, we demonstrate here that the stratification is also acutely sensitive to the mesoscale eddy energy dissipation time-scale. Within the context of a global ocean circulation model with an energy constrained mesoscale eddy parameterization, it is shown that modest variations in the eddy energy dissipation time-scale lead to significant variations in key metrics relating to ocean circulation, namely the Antarctic Circumpolar Current transport, Atlantic Meridional Overturning Circulation strength, and global ocean heat content, over long time-scales. The results highlight a need to constrain uncertainties associated with eddy energy dissipation for climate model projections over centennial time-scales, but also for paleoclimate simulations over millennial time-scales.

Plain Language Summary

Modest uncertainties in mesoscale eddy energy dissipation time-scale translate to significant variations in the global ocean circulation and heat content on long time-scales. A 50% change in the eddy energy dissipation time-scale has a similar effect to halving and doubling of Southern Ocean wind stress in quasi-equilibrium calculations, leading to a global ocean heat content change that is an order of magnitude larger than those typically found in modern day era reconstructions and projections. The results highlight a need to combine theoretical, modeling, and observational efforts to constrain the uncertainties in eddy energy dissipation for climate projections and paleoclimate reconstructions.

1 Overview and key findings

Evolution of the ocean stratification plays a fundamental role in climate evolution, through the associated consequences for the global meridional overturning circulation. Reconstructions of past climate together with the use of numerical models have highlighted how shoaling and weakening of the Atlantic Meridional Overturning Circulation (AMOC), associated with changes in the deep/abyssal stratification, have important consequences for the global energy, oxygen and carbon cycles (e.g., Zhang & Vallis, 2013; Adkins, 2013; Ferrari et al., 2014; Burke et al., 2015; Bopp et al., 2017; Jansen, 2017; Takano et al., 2018; Galbraith & de Lavergne, 2019). In particular, the Southern Ocean is “*disproportionately important*” (Newman et al., 2019) for the global stratification profiles because of the connection in the stratification profiles, with the implication that Southern Ocean processes can exert a control on the global overturning circulation.

It is known that the Southern Ocean stratification is primarily dependent on wind forcing (Toggweiler & Samuels, 1995; Toggweiler et al., 2006), buoyancy forcing (Hogg, 2010; Morrison et al., 2011; Jansen, 2017), and to eddy dynamics (Munday et al., 2013; Farneti et al., 2015; Bishop et al., 2016). Focusing on mesoscale eddies, an extra complication arises since there are notable divergences in model response depending on how mesoscale eddies are represented, between whether they are represented explicitly or parameterized (Munday et al., 2013; Farneti et al., 2015; Bishop et al., 2016), and the form of the parameterization (Hofman & Morales Maqueda, 2011; Viebahn & Eden, 2012; Meredith et al., 2012; Munday et al., 2013; Farneti et al., 2015; Bishop et al., 2016). While the issue of mesoscale eddy representation “*frequently have a larger effect on ocean climate sensitivity than the total effect of other classes of parameterizations*” (Fox-Kemper et al., 2019), there have been advances on the eddy parameterization aspect, where the role of eddy energy in mesoscale eddy parameterizations is increas-

ingly being studied (Eden & Greatbatch, 2008; Marshall & Adcroft, 2010; Marshall et al., 2012; Eden et al., 2014). Models with parameterized eddies employing eddy energy constrained eddy diffusivities or transport coefficients display improved model responses that are closer to the responses displayed in analogous high resolution models (Jansen & Held, 2014; Jansen, Held, et al., 2015; Jansen, Adcroft, et al., 2015; Mak et al., 2017, 2018; Klöwer et al., 2018; Bachman, 2017). In particular, the GEOMETRIC parameterization (Marshall et al., 2012; Mak et al., 2017; Marshall et al., 2017; Mak et al., 2018) — effectively rescaling the standard Gent–McWilliams (Gent & McWilliams, 1990; Gent et al., 1995) eddy transport coefficient by the total eddy energy according to rigorous mathematical identities (Marshall et al., 2012; Maddison & Marshall, 2013) and supported in diagnoses of eddy resolving calculations (Bachman et al., 2017) — imparts an Antarctic Circumpolar Current and Atlantic Meridional Overturning Circulation sensitivity to changes in the Southern Ocean wind forcing to idealized ocean climate models that are closer the analogous high resolution models (Mak et al., 2018).

A natural question to ask is how strong is the influence of mesoscale eddy dynamics on the Southern Ocean as well as global ocean circulation. Since there is a link between eddy energy and the degree of feedback arising from the eddies, the mesoscale eddy energy dissipation time-scale should therefore play an important role: if more energy is drained from the mesoscale eddy field, the associated eddy form stress weakens, thereby reducing vertical momentum transport, in turn modifying the momentum balance. Following this line of argument, it was argued in Marshall et al. (2017) that the overall circumpolar transport in the Southern Ocean should increase with increasing eddy energy dissipation, and so, by thermal wind shear relation, lead to steeply tilting isopycnals in the Southern and ocean and a deepening of the global pycnocline depth over long time-scales.

The extent of the influence of eddy energy dissipation on the global circulation is the primary focus of the present work. A key finding here is that a 50% variation around a control time-scale has a similar effect to halving and doubling of the present day Southern Ocean wind stress on the modeled Antarctic Circumpolar Current transport, Atlantic Meridional Overturning Circulation strength, and the global integrated ocean heat content anomaly (Fig. 1 and Fig. 3), attributed primarily to changes in the global pycnocline depth. While the Southern Ocean wind forcing is not expected to vary so dramatically, the extent of plausible mesoscale eddy energy dissipation time-scale is not known, due to a lack of theoretical and observation constraints currently available. The results here thus highlight a crucial need to combine theoretical, modeling, and observational efforts to constrain the uncertainties in eddy energy dissipation, not only from a theoretical point of view for understanding, but also for practical purposes in constraining uncertain model parameters for numerical models used in climate projections and paleoclimate reconstructions.

2 Method and model description

The principal focus here is on quasi-equilibrium sensitivities of the global overturning circulation to the eddy energy dissipation time-scale. While one might consider employing an eddy resolving ocean model for such a study, the associated computational costs are prohibitive. Thus we employ a model with parameterized eddies, and utilize the Nucleus for European Modelling of the Ocean (NEMO, v3.7dev r8666) (Madec, 2008) in the global configuration (ORCA) with realistic bathymetry, employing the tri-polar ORCA grid (Madec & Imbard, 1996) and the LIM3 ice model (Rousset et al., 2015). The present ORCA1 model has a nominal horizontal resolution of 1° , employs 46 uneven vertical levels, and is initialized with WOA13 climatology (Locarnini et al., 2013; Zweng et al., 2013). The model employs the TEOS-10 equation of state (Roquet et al., 2015), with the atmospheric forcing modeled by the NCAR

bulk formulae with normal year forcing (Large & Yeager, 2009). Sea surface salinity but not temperature restoration is included to reduce model drift.

An energetically constrained mesoscale eddy parameterization scheme is required, and for our investigation the GEOMETRIC parameterization for mesoscale eddies (Marshall et al., 2012; Mak et al., 2018) was chosen and implemented in NEMO (see Supplementary Information for implementation details). Briefly, GEOMETRIC computes a horizontally and temporally varying coefficient for eddy induced advection (Gent & McWilliams, 1990; Gent et al., 1995) according to (cf. Eq. 4 of Mak et al., 2018)

$$\kappa_{\text{gm}} = \alpha \frac{\int E \, dz}{\int (M^2/N) \, dz}, \quad (1)$$

where M and N are the horizontal and vertical buoyancy frequencies, α is a non-dimensional tuning parameter (bounded in magnitude by 1), and E is the total (potential and kinetic) eddy energy. The depth-integrated eddy energy $\int E \, dz$ is provided by a parameterized eddy energy budget given by (cf. Eq. 2 of Mak et al., 2018)

$$\frac{d}{dt} \int E \, dz + \underbrace{\nabla_H \cdot \left((\tilde{\mathbf{u}}^z - |c| \mathbf{e}_x) \int E \, dz \right)}_{\text{advection}} = \underbrace{\int \kappa_{\text{gm}} \frac{M^4}{N^2} \, dz}_{\text{source}} - \underbrace{\lambda \int (E - E_0) \, dz}_{\text{dissipation}} + \underbrace{\eta_E \nabla_H^2 \int E \, dz}_{\text{diffusion}} \quad (2)$$

The depth-integrated eddy energy is advected by the depth average flow $\tilde{\mathbf{u}}^z$ and propagated westward at the long Rossby wave phase speed $|c|$ (Chelton et al., 2011; Klocker & Marshall, 2014), has growth arising from slumping of mean density surfaces, and diffused in the horizontal (Grooms, 2015; Ni, Zhai, Wang, & Marshall, 2020; Ni, Zhai, Wang, & Hughes, 2020), with ∇_H denoting the horizontal gradient operator and the η_E the associated eddy energy diffusivity. A linear dissipation of eddy energy at rate λ (but maintaining a minimum eddy energy level E_0) is utilized, so λ^{-1} is the eddy energy dissipation time-scale. For this work, $\alpha = 0.04$ is prescribed, partially informed by the results of Poulsen et al. (2019), and $\eta_E = 500 \text{ m}^2 \text{ s}^{-1}$ was chosen. While the Gent–McWilliams coefficient follows the prescription given in Eq. 1, the isoneutral diffusion coefficient (Griffies, 1998) is kept constant at $1000 \text{ m}^2 \text{ s}^{-1}$. Values of the isopycnal slopes used to compute the parameterized eddy energy, eddy induced advection and isoneutral diffusion are limited to $1/100$ in the interior, and linearly decreased from the base of the model mixed layer to zero at the surface to maintain no flux conditions. For more details of the GEOMETRIC parameterization and its implementation in NEMO, please see the Supporting Information.

Given the lack of constraints on the values and uncertainties associated with the eddy energy dissipation time-scale, for simplicity we take the eddy energy dissipation time-scale λ^{-1} to be a constant in space and time, with a control value of $\lambda^{-1} = 100$ days (e.g., Melet et al., 2015, Marshall & Zhai, pers. comm.), and consider a range of values spanning approximately 50% about the control value (in this case six experiments with λ^{-1} ranging 60 to 160 days in increments of 20 days). A control model utilizing $\lambda^{-1} = 100$ days was first spun up for 1500 years, after which the perturbation experiments were integrated for a further 1600 years; see Supplementary Information Fig. S1-4 for some of the resulting climatology. All metrics presented in this work were diagnosed from data averaged over the last 100 model years.

3 Results

3.1 Sensitivity to eddy energy dissipation time-scale

The key metrics of interest here are the total Antarctic Circumpolar Current (ACC) transport, Atlantic Meridional Overturning Circulation (AMOC) strength, and the globally integrated Ocean Heat Content (OHC) anomaly relative to the control

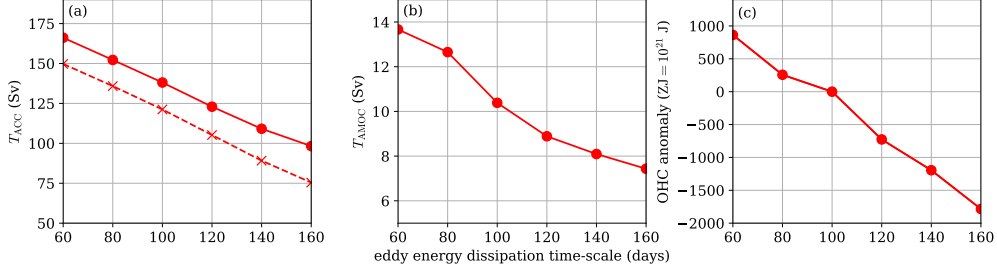


Figure 1. Diagnostics from the varying eddy energy dissipation time-scale experiments. Diagnostics are: (a) ACC transport (total in solid lines, thermal wind component in dashed lines); (b) AMOC strength; (c) domain-integrated ocean heat content anomalies as solid lines, where the anomalies are relative to the control calculation (one times wind amplification and dissipation time-scale of 100 days) with the value of 21,300 ZJ.

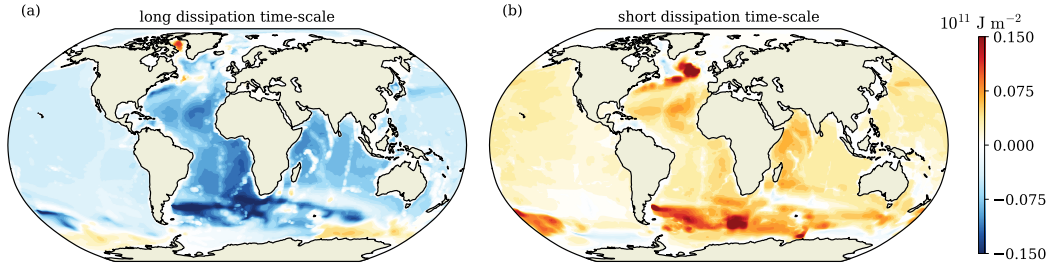


Figure 2. Depth-integrated ocean heat content anomaly (relative to the control calculation with dissipation time-scale of 100 days and one times wind amplification) for varying dissipation experiments (a, b, at $\lambda^{-1} = 160$ and 60 days respectively).

calculation, respectively given as the transport through the model Drake passage, the transport over the top 1000 m at the model 26° N on the Western side of the Atlantic, and the global integrated conservative temperature multiplied accordingly by the density and heat capacity. Fig. 1 compares these metrics diagnosed from experiments varying the eddy energy dissipation time-scale. Increasing the dissipation time-scale (i.e., decreased damping of the eddies) leads to a substantial decrease in the ACC transport, AMOC strength, and total ocean heat content anomaly, which can be attributed to the deepening of the global pycnocline, consistent with theoretical arguments (Marshall et al., 2017). In particular, we note that the changes in the OHC anomalies found in post-industrial period reconstructions (Levitus et al., 2012; Cheng et al., 2017, 2019; Zanna et al., 2019) are typically on the order of 10^{23} J (100 ZJ), while the changes to total OHC associated with the uncertainties in eddy energy dissipation time-scale here can be an order of magnitude larger (10^{24} J).

The distribution of the lateral depth-integrated ocean heat content for varying eddy energy dissipation time-scale is shown in Fig. 2. Varying the eddy energy dissipation time-scale leads to a significant global change in the OHC anomalies, attributed mainly to the changes in pycnocline depth (Supporting Information, Fig. S6-9). Note also that the changes appear to be most significant over the Southern Ocean and in the Atlantic basin, attributed to significant changes in the AMOC as well as the overturning within the Southern Ocean (Supporting Information, Fig. S3-4).

Here, changing the eddy energy dissipation time-scale λ^{-1} affects the total eddy energy E , which in turn impacts the Gent–McWilliams coefficient κ_{gm} . While the significant changes to global OHC and circulation arising from changing κ_{gm} has been noted before (e.g. Zhang & Vallis, 2013), the fundamental difference here is that the sensitivities are arising through uncertainties in the eddy energy dissipation that happens to impact the Gent–McWilliams parameter, and the eddy energy dissipation is a process that in principle is perhaps more amenable to be constrained by theoretical, numerical or observational means.

3.2 Sensitivity to Southern Ocean wind forcing

For completeness, experiments varying Southern Ocean wind forcing were also performed. The zonal wind stress over the Southern Ocean region within the model is amplified instead of the imposed zonal wind speed, so that any modifications to the ocean surface evaporation and turbulent fluxes as calculated through the bulk formulae occurs through changes to the ocean state rather than the imposed wind forcing. Two sets of perturbation experiments were performed: (a) a κ_{gm} that is varying in the horizontal and in time as given by Eq. 1, with no further re-tuning (denoted GEOM), and (b) a prescribed κ_{gm} diagnosed from the last 100 years of the control spin-up (denoted GM), but one that is now time-independent although still spatially varying.

Fig. 3 shows the sensitivities of the same global ocean climatological metrics to changes in the imposed Southern Ocean wind forcing. In Fig. 3(a), while the total ACC transport (solid lines) increases with wind forcing, the ACC thermal wind transport (dashed lines) in the GEOM calculations (orange lines, cross markers) is relatively insensitive to changes in the wind forcing, demonstrating the eddy saturation phenomenon (Hallberg & Gnanadesikan, 2006; Meredith & Hogg, 2006; Munday et al., 2013; Farneti et al., 2015; Bishop et al., 2016). On the other hand, the corresponding AMOC strength shown in Fig. 3(b) in the GEOM calculations display a reduced sensitivity to changes in the Southern Ocean wind forcing relative to the GM case, and is related to the phenomenon of eddy compensation (Gent & Danabasoglu, 2011; Hofman & Morales Maqueda, 2011; Viebahn & Eden, 2012; Meredith et al., 2012; Munday et al., 2013; Farneti et al., 2015; Bishop et al., 2016). The aforementioned sensitivities coincide with a weaker sensitivity of the global pycnocline depth to changes in Southern Ocean wind forcing (Marshall et al., 2017; Mak et al., 2018). Comparing Fig. 3 with Fig. 1, a 50% change about a chosen eddy energy dissipation time-scale has a comparable effect to halving or doubling the Southern Ocean wind forcing in the diagnosed metrics. As with the varying eddy energy dissipation experiments, the OHC anomalies are particularly significant over the Southern Ocean and the Atlantic basin (Supporting Information, Fig. S5). In the present case of varying wind stress, however, the notable variations in the OHC anomalies are attributed to significant changes in the abyssal watermass properties (Supporting Information, Fig. S6-9). The observed changes in the watermass properties may perhaps be attributed to a modified sea ice extent (Supporting Information, Fig. S10) via changes in the sea ice export by the wind, leading to changes in deep water formation and abyssal watermass properties, analogous to the mechanism proposed in Ferrari et al. (2014) and Burke et al. (2015).

4 Summary and outlooks

The present work demonstrates that, within the context of a global configuration ocean model with an energetically constrained mesoscale eddy parameterization, modest and perhaps not implausible variations in the mesoscale eddy energy dissipation time-scale translate to significant sensitivities of the diagnosed Antarctic Circumpolar Current transport, Atlantic Meridional Overturning Circulation strength, and the global Ocean Heat Content over long time-scales in the modeled ocean. The physi-

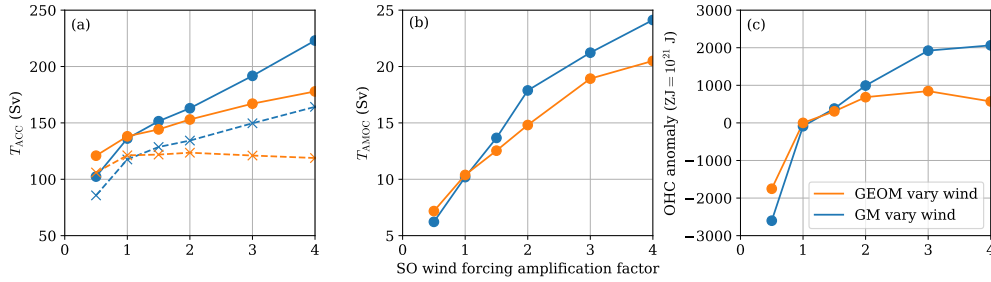


Figure 3. Diagnostics from the varying Southern Ocean wind stress experiments (with GEOM and GM calculations in orange and blue respectively), showing: (a) ACC transport (total in solid lines, thermal wind component in dashed lines); (b) AMOC strength; (c) domain-integrated ocean heat content anomaly, where the anomalies are relative to the respective control calculations (one times wind amplification and dissipation time-scale of 100 days) with the value of 21,300 ZJ.

cal reasons for the sensitivity is that modifying the eddy energy dissipation leads to changes in the mesoscale eddy dynamics in the Southern Ocean, that in turn lead to significant changes to the global ocean stratification over long time-scales. The sensitivity of the aforementioned key ocean climatological metrics to eddy energy dissipation time-scale is found to be comparable to those found for varying Southern Ocean wind forcing, where a 50% change about a chosen eddy energy dissipation time-scale has a comparable effect to halving or doubling the Southern Ocean wind forcing in the diagnosed ocean circulation metrics. In particular, changes to the globally integrated Ocean Heat Content anomalies can vary by up to an order of magnitude larger than for reconstructions for total ocean heat content for the anthropogenic period (Levitus et al., 2012; Cheng et al., 2017, 2019; Zanna et al., 2019), and comparable to the end of 21st projections under the Representative Concentration Pathways scenarios (see figure in Cheng et al., 2019). While the changes in the Southern Ocean wind forcing are not expected to vary to the extent considered in this work (e.g. Lin et al., 2018), there are no strong theoretical, numerical or observational constraints on the eddy energy dissipation time-scale and its distribution (but see next paragraph on works towards constraining the energy fluxes of the contributing processes). There is thus a need to combine and dedicate theoretical, modeling and observational efforts to constrain the uncertainties in the eddy energy dissipation time-scale, given the impact the associated uncertainties can have.

In the present work the eddy energy dissipation is linear (cf., Klymak, 2018) with a time-scale that is a prescribed constant in space and time. One particular consequence of a prescribed spatially constant eddy energy dissipation time-scale may be seen in Fig. 4, which shows the total (kinetic and potential) eddy energy diagnosed from a high-resolution global configuration model and from the control experiment here. While the eddy energy signature displays some similarities in terms of spatial patterns in the Southern Ocean and Western Boundary Current regions, there is clearly room for improvement for the parameterized case. For example, the eddy energy signature in the parameterized case is too weak in the Western Boundary Currents and in the equatorial region, attributed to the fact that the spatially constant eddy energy dissipation time-scale was chosen somewhat with the Southern Ocean in mind, and is probably too short for the ocean basin regions (Marshall & Zhai, pers. comm.). The mesoscale eddy energy dissipation time-scale is expected to be a more complicated function than the choice taken here and, fundamentally, should depend on a wide

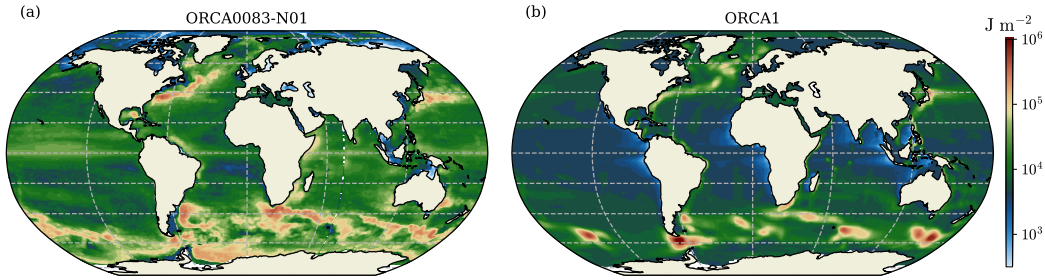


Figure 4. Depth-integrated total (kinetic and potential) eddy energy density (in units of J m^{-2}), diagnosed from (a) the high resolution ORCA0083-N01 calculation with explicit eddies, and (b) from the GEOM control calculation.

variety of dynamical processes such as bottom drag (e.g. Sen et al., 2008; Ruan et al., 2021), non-propagating form drag (Klymak, 2018; Klymak et al., 2021), return to mean-flow (e.g. Bachman, 2017; Jansen et al., 2019) scattering into internal waves (e.g. Nikurashin et al., 2013; Melet et al., 2015; MacKinnon et al., 2017; Yang et al., 2018; Sutherland et al., 2019), loss of balance (e.g. Molemaker et al., 2005; Barkan et al., 2017; Rocha et al., 2018), and eddy killing by the wind (e.g. Xu et al., 2016; Rai et al., 2021). Though the challenges in constraining the uncertainties in the eddy energy dissipation time-scale are formidable, the observed/diagnosed eddy energy signature can perhaps act as a target towards efforts to constrain the aforementioned unknowns, highlighting the potential for further research relating to ocean energetic pathways and its consequences for climate evolution (see for example Ruan et al. (2021) for a recent review of research relating to ocean eddy energy pathways).

While the present results are based on the choice of utilizing the GEOMETRIC parameterization for mesoscale eddies (Mak et al., 2018), given the link of the eddy energy dissipation time-scale and the resulting eddy induced circulation through the eddy energy (in this work through the Gent–McWilliams coefficient for eddy induced advection), the sensitivities of key ocean climatological metrics to the eddy energy dissipation is expected to carry over if other eddy energy based parameterization schemes for mesoscale eddies (e.g. Jansen, Adcroft, et al., 2015; Bachman, 2017) are utilized, or if analogous experiments are carried out in global eddy resolving models varying possible mechanisms of mesoscale eddy energy dissipation (e.g. bottom drag, cf. Marshall et al., 2017), although the magnitude of the sensitivities may differ. While the present work focused on quasi-equilibrium calculations, similar conclusions but with reduced magnitudes of the sensitivities are expected for centennial time-scale calculations. What is clear, however, is that the present work has significant consequences for paleoclimate simulations involving the ocean, such as Paleoclimate Modelling Intercomparison Project calculations (PMIP, Kageyama et al., 2018), given the long time-scales inherently required for the related simulations. Potential impact assessment for climate projections and paleoclimate simulations in light of the present work will be investigated and reported in due course.

Acknowledgments

This work was funded by the UK Natural Environment Research Council grant NE/R000999/1 and utilized the ARCHER UK National Supercomputing Service. JM also acknowledges financial support from the RGC Early Career Scheme 2630020 and the Center for Ocean Research in Hong Kong and Macau, a joint research center be-

tween the Qingdao National Laboratory for Marine Science and Technology and Hong Kong University of Science and Technology. The data used for generating the plots in this article is available through <http://dx.doi.org/10.5281/zenodo.5732755>. The authors would like to thank Andrew Coward for providing access to the ORCA0083-N01 dataset through the ARCHER RDF service, Xiaoming Zhai for discussions relating to eddy energy data, and George Nurser for discussions in relation to the GEOMETRIC implementation and outlooks.

References

- Adkins, J. F. (2013). The role of deep ocean circulation in setting glacial climates. *Paleoceanography*, *28*, 539–561. doi: 10.1002/palo.20046
- Bachman, S. D. (2017). The GM+E closure: A framework for coupling backscatter with the Gent and McWilliams parameterization. *Ocean Modell.*, *136*, 85–106. doi: 10.1016/j.ocemod.2019.02.006
- Bachman, S. D., Marshall, D. P., Maddison, J. R., & Mak, J. (2017). Evaluation of a scalar transport coefficient based on geometric constraints. *Ocean Modell.*, *109*, 44–54. doi: 10.1016/j.ocemod.2016.12.004
- Barkan, R., Winters, K. B., & McWilliams, J. C. (2017). Stimulated imbalance and the enhancement of eddy kinetic energy dissipation by internal waves. *J. Phys. Oceanogr.*, *47*, 181–198. doi: 10.1175/JPO-D-16-0117.1
- Bishop, S. P., Gent, P. R., Bryan, F. O., Thompson, A. F., Long, M. C., & Abernathy, R. P. (2016). Southern Ocean overturning compensation in an eddy-resolving climate simulation. *J. Phys. Oceanogr.*, *46*, 1575–1592. doi: 10.1175/JPO-D-15-0177.1
- Bopp, L., Roesch, L., Untersee, A., Le Mezo, P., & Kageyama, M. (2017). Ocean (de)oxygenation from the Last Glacial Maximum to the twenty-first century: insights from Earth System models. *Phil. Trans. R. Soc. A*, *375*, 20160323. doi: 10.1098/rsta.2016.0323
- Burke, A., Stewart, A. L., Adkins, J. F., Ferrari, R., Jansen, M. F., & Thompson, A. F. (2015). The glacial mid-depth radiocarbon bulge and its implications for the overturning circulation. *Paleoceanography*, *30*, 1021–1039. doi: 10.1002/2015PA002778
- Chelton, D. B., Schlax, M. G., & Samelson, R. M. (2011). Global observations of nonlinear mesoscale eddies. *Prog. Oceanogr.*, *91*, 167–216. doi: 10.1016/j.pocean.2011.01.002
- Cheng, L., Abraham, J., Hausfather, Z., & Trenberth, K. E. (2019). How fast are the oceans warming? *Sci. Adv.*, *363*, 128–129. doi: 10.1126/science.aav7619
- Cheng, L., Trenberth, K. E., Fasullo, J., Boyer, T., Abraham, J., & Zhu, J. (2017). Improved estimates of ocean heat content from 1960 to 2015. *Sci. Adv.*, *3*, e1601545. doi: 10.1126/sciadv.1601545
- Eden, C., Czeschel, L., & Olbers, D. (2014). Toward energetically consistent ocean models. *J. Phys. Oceanogr.*, *44*, 3160–3184. doi: 10.1016/JPO-D-13-0260.1
- Eden, C., & Greatbatch, R. J. (2008). Towards a mesoscale eddy closure. *Ocean Modell.*, *20*, 223–239. doi: 10.1016/j.ocemod.2007.09.002
- Farneti, R., Downes, S. M., Griffies, S. M., Marsland, S. J., Behrens, E., Bentsen, M., ... Yeager, S. G. (2015). An assessment of Antarctic Circumpolar Current and Southern Ocean meridional overturning circulation during 1958–2007 in a suite of interannual CORE-II simulations. *Ocean Modell.*, *94*, 84–120. doi: 10.1016/j.ocemod.2015.07.009
- Ferrari, R., Jansen, M. F., Adkins, J. F., Burke, A., Stewart, A. L., & Thompson, A. F. (2014). Antarctic sea ice control on ocean circulation in present and glacial climates. *Proc. Natl Acad. Sci. USA*, *111*(24), 8753–8758. doi: 10.1073/pnas.1323922111
- Fox-Kemper, B., Adcroft, A. J., Böning, C. W., Chassignet, E. P., Curchitser, E. N.,

- Danabasoglu, G., . . . Yeager, S. G. (2019). Challenges and prospects in ocean circulation models. *Front. Mar. Sci.*, *6*, 65. doi: 10.3389/fmars.2019.00065
- Galbraith, E., & de Lavergne, C. (2019). Response of a comprehensive climate model to a broad range of external forcings: relevant for deep ocean ventilation and the development of late Cenozoic ice ages. *Clim. Dyn.*, *52*, 623–679. doi: 10.1007/s00382-018-4157-8
- Gent, P. R., & Danabasoglu, G. (2011). Response to increasing southern hemisphere winds in CCSM4. *J. Climate*, *24*, 4992–4998. doi: 10.1175/JCLI-D-10-05011.1
- Gent, P. R., & McWilliams, J. C. (1990). Isopycnal mixing in ocean circulation models. *J. Phys. Oceanogr.*, *20*, 150–155. doi: 10.1175/1520-0485(1990)020<0150:IMIOCM>2.0.CO;2
- Gent, P. R., Willebrand, J., McDougall, T. J., & McWilliams, J. C. (1995). Parameterizing eddy-induced tracer transports in ocean circulation models. *J. Phys. Oceanogr.*, *25*, 463–474. doi: 10.1175/1520-0485(1995)025<0463:PEITTI>2.0.CO;2
- Griffies, S. M. (1998). The Gent–McWilliams skew flux. *J. Phys. Oceanogr.*, *28*, 831–841. doi: 10.1175/1520-0485(1998)028<0831:TGMSF>2.0.CO;2
- Grooms, I. (2015). A computational study of turbulent kinetic energy transport in barotropic turbulence on the f -plane. *Phys. Fluids*, *27*, 101701. doi: 10.1063/1.4934623
- Hallberg, R., & Gnanadesikan, A. (2006). The role of eddies in determining the structure and response of the wind-driven Southern Hemisphere overturning: Results from the Modeling Eddies in the Southern Ocean (MESO) projects. *J. Phys. Oceanogr.*, *36*, 2232–2252. doi: 10.1175/JPO2980.1
- Hofman, M., & Morales Maqueda, M. A. (2011). The response of Southern Ocean eddies to increased midlatitude westerlies: A non-eddy resolving model study. *Geophys. Res. Lett.*, *38*, L03605. doi: 10.1029/2010GL045972
- Hogg, A. M. (2010). An Antarctic Circumpolar Current driven by surface buoyancy forcing. *Geophys. Res. Lett.*, *37*, L23601. doi: 10.1029/2010GL044777
- Jansen, M. F. (2017). Glacial ocean circulation and stratification explained by reduced atmospheric temperature. *Proc. Natl Acad. Sci. USA*, *114*(1), 45–50. doi: 10.1073/pnas.1610438113
- Jansen, M. F., Adcroft, A., Khani, S., & Kong, H. (2019). Toward an energetically consistent, resolution aware parameterization of ocean mesoscale eddies. *J. Adv. Model. Earth Syst.*, *1*, 1–17. doi: 10.1029/2019MS001750
- Jansen, M. F., Adcroft, A. J., Hallberg, R., & Held, I. M. (2015). Parameterization of eddy fluxes based on a mesoscale energy budget. *Ocean Modell.*, *92*, 28–41. doi: 10.1016/j.ocemod.2015.05.007
- Jansen, M. F., & Held, I. M. (2014). Parameterizing subgrid-scale eddy effects using energetically consistent backscatter. *Ocean Modell.*, *80*, 36–48. doi: 10.1016/j.ocemod.2014.06.002
- Jansen, M. F., Held, I. M., Adcroft, A. J., & Hallberg, R. (2015). Energy budget-based backscatter in an eddy permitting primitive equation model. *Ocean Modell.*, *92*, 15–26. doi: 10.1016/j.ocemod.2015.07.015
- Kageyama, M., Braconnot, P., Harrison, S. P., Haywood, A. M., Jungclaus, J. H., Otto-Bliesner, B. L., . . . Zhou, T. (2018). The PMIP4 contribution to CMIP6 – Part 1: Overview and over-arching analysis plan. *Geosci. Model Dev.*, *11*(3), 1033–1057. doi: 10.5194/gmd-11-1033-2018
- Klocker, A., & Marshall, D. P. (2014). Advection of baroclinic eddies by depth mean flow. *Geophys. Res. Lett.*, *41*, L060001. doi: 10.1002/2014GL060001
- Klöwer, M., Jansen, M. F., Claus, M., Greatbatch, R. J., & Thomsen, S. (2018). Energy budget-based backscatter in a shallow water model of a double gyre basin. *Ocean Modell.*, *132*, 1–11. doi: 10.1016/j.ocemod.2018.09.006
- Klymak, J. (2018). Non-propagating form drag and turbulence due to stratified flow

- over large-scale abyssal hill topography. *J. Phys. Oceanogr.*, *48*, 2383–2395. doi: 10.1175/JPO-D-17-0225.1
- Klymak, J., Balwada, D., Naveira Garabato, A. C., & Abernathey, R. (2021). Parameterizing nonpropagating form drag over rough bathymetry. *J. Phys. Oceanogr.*, *51*, 1489–1501. doi: 10.1175/JPO-D-20-0112.1
- Large, W. G., & Yeager, S. (2009). The global climatology of an interannually varying air-sea flux data set. *Clim. Dynam.*, *33*, 341–364. doi: 10.1007/s00382-008-0441-3
- Levitus, S., Antonov, J. I., Boyer, T. P., Baranova, O. K., Garcia, H. E., Locarnini, R. A., ... Zweng, M. M. (2012). Work ocean hat content and thermosteric sea level change (0–2000 m), 1955–2010. *Geophys. Res. Lett.*, *39*, L10603. doi: 10.1029/2012GL051106
- Lin, X., Zhai, X., Wang, Z., & Munday, D. R. (2018). Mean, variability, and trend of Southern Ocean wind stress: Role of wind fluctuations. *J. Climate*, *31*, 3557–3573. doi: 10.1175/JCLI-D-17-0481.1
- Locarnini, R. A., Mishonov, A. V., Antonov, J. I., Boyer, T. P., Garcia, H. E., Baranova, O. K., ... Seidov, D. (2013). World Ocean Atlas 2013, Volume 1: Temperature. In S. Levitus (Ed.), *Noaa atlas nesdis 73* (pp. 1–40).
- MacKinnon, J. A., Alford, M. H., Ansong, J. K., Arbic, B. K., Barna, A., Briegleb, B. P., ... Zhao, Z. (2017). Climate process team on internal-wave driven ocean mixing. *J. Fluid Mech.*, *98*, 2429–2454. doi: 10.1175/BAMS-D-16-0030.1
- Maddison, J. R., & Marshall, D. P. (2013). The Eliassen–Palm flux tensor. *J. Fluid Mech.*, *729*, 69–102. doi: 10.1017/jfm.2013.259
- Madec, G. (2008). NEMO ocean engine. *Note du Pôle de modélisation, Institut Pierre-Simon Laplace (IPSL), No. 27*.
- Madec, G., & Imbard, M. (1996). A global ocean mesh to overcome the North Pole singularity. *Clim. Dyn.*, *12*, 381–388. doi: 10.1007/BF00211684
- Mak, J., Maddison, J. R., Marshall, D. P., & Munday, D. R. (2018). Implementation of a geometrically informed and energetically constrained mesoscale eddy parameterization in an ocean circulation model. *J. Phys. Oceanogr.*, *48*, 2363–2382. doi: 10.1175/JPO-D-18-0017.1
- Mak, J., Marshall, D. P., Maddison, J. R., & Bachman, S. D. (2017). Emergent eddy saturation from an energy constrained parameterisation. *Ocean Modell.*, *112*, 125–138. doi: 10.1016/j.ocemod.2017.02.007
- Marshall, D. P., & Adcroft, A. J. (2010). Parameterization of ocean eddies: Potential vorticity mixing, energetics and Arnold’s first stability theorem. *Ocean Modell.*, *32*, 1571–1578. doi: 10.1016/j.ocemod.2010.02.001
- Marshall, D. P., Ambaum, M. H. P., Maddison, J. R., Munday, D. R., & Novak, L. (2017). Eddy saturation and frictional control of the Antarctic Circumpolar Current. *Geophys. Res. Lett.*, *44*, 286–292. doi: 10.1002/2016GL071702
- Marshall, D. P., Maddison, J. R., & Berloff, P. S. (2012). A framework for parameterizing eddy potential vorticity fluxes. *J. Phys. Oceanogr.*, *42*, 539–557. doi: 10.1175/JPO-D-11-048.1
- Melet, A., Hallberg, R., Adcroft, A., Nikurashin, M., & Legg, S. (2015). Energy flux into internal lee waves: Sensitivity to future climate changes using linear theory and a climate model. *J. Climate*, *28*, 2365–2384. doi: 10.1175/JCLI-D-14-00432.1
- Meredith, M. P., Garabato, A. C. N., Hogg, A. M., & Farneti, R. (2012). Sensitivity of the overturning circulation in the Southern Ocean to decadal changes in wind forcing. *J. Climate*, *25*, 99–110. doi: 10.1175/2011JCLI4204.1
- Meredith, M. P., & Hogg, A. M. (2006). Circumpolar response of Southern Ocean eddy activity to a change in the Southern Annular Mode. *Geophys. Res. Lett.*, *33*, L16608.
- Molemaker, M. J., McWilliams, J. C., & Yavneh, I. (2005). Baroclinic instability and loss of balance. *J. Phys. Oceanogr.*, *35*, 1505–1517. doi: 10.1175/JPO2770

.1

- Morrison, A. K., Hogg, A. M., & Ward, M. L. (2011). Sensitivity of the Southern Ocean overturning circulation to surface buoyancy forcing. *Geophys. Res. Lett.*, *38*, L14602. doi: 10.1029/2011GL048031
- Munday, D. R., Johnson, H. L., & Marshall, D. P. (2013). Eddy saturation of equilibrated circumpolar currents. *J. Phys. Oceanogr.*, *43*, 507–532. doi: 10.1175/JPO-D-12-095.1
- Newman, L., Heil, P., Trebilco, R., Katsumata, K., Constable, A., van Wijk, E., . . . Spreen, G. (2019). Delivering sustained, coordinated, and integrated observations of the Southern Ocean for global impact. *Front. Mar. Sci.*, *6*, 433. doi: 10.3389/fmars.2019.00433
- Ni, Q., Zhai, X., Wang, G., & Hughes, C. W. (2020). Widespread mesoscale dipoles in the global ocean. *J. Geophys. Res. Oceans*, *125*, e2020JC016479. doi: 10.1029/2020JC016479
- Ni, Q., Zhai, X., Wang, G., & Marshall, D. P. (2020). Random movement of mesoscale eddies in the global ocean. *J. Phys. Oceanogr.*, *50*, 2341–2357. doi: 10.1175/JPO-D-19-0192.1
- Nikurashin, M., Vallis, G. K., & Adcroft, A. (2013). Routes to energy dissipation for geostrophic flows in the Southern Ocean. *Nature Geosci.*, *6*, L08610. doi: 10.1038/NGEO1657
- Poulsen, M. B., Jochum, M., Maddison, J. R., Marshall, D. P., & Nuterman, R. (2019). A geometric interpretation of Southern Ocean eddy form stress. *J. Phys. Oceanogr.*, *49*, 2553–2570. doi: 10.1175/JPO-D-18-0220.1
- Rai, S., Hecht, M., Maltrud, M. E., & Aluie, H. (2021). Scale of oceanic eddy killing by wind from global satellite observations. *Sci. Adv.*, *7*, eabf4920. doi: 10.1126/sciadv.abf4920
- Rocha, C. B., Wagner, G. L., & Young, W. R. (2018). Stimulated generation: extraction of energy from balanced flow by near-inertial waves. *J. Fluid Mech.*, *847*, 417–451. doi: 10.1017/jfm.2018.308
- Roquet, F., Madec, G., McDougall, T. J., & Barker, P. M. (2015). Accurate polynomial expressions for the density and specific volume of seawater using the TEOS-10 standard. *Ocean Modell.*, *90*, 29–43. doi: 10.1016/j.ocemod.2015.04.002
- Rousset, C., Vancoppenolle, M., Madec, G., Fichefet, T., Flavoni, S., Barthélemy, A., . . . Vivier, F. (2015). The Louvain-La-Neuve sea ice model LIM3.6: global and regional capabilities. *Geosci. Model Dev.*, *8*, 2991–3005. doi: 10.5194/gmd-8-2991-2015
- Ruan, X., Wenegrat, J. O., & Gula, J. (2021). Slippery bottom boundary layers: The loss of energy from the general circulation by bottom drag. *Geophys. Res. Lett.*, *48*, e2021GL094434. doi: 10.1029/2021GL094434
- Sen, A., Scott, R. B., & Arbic, B. K. (2008). Global energy dissipation rate of deep-ocean low-frequency flows by quadratic bottom boundary layer drag: Computations from current-meter data. *Geophys. Res. Lett.*, *35*, L09606. doi: 10.1029/2008GL033407
- Sutherland, B. R., Achatz, U., Caulfield, C. P., & Klymak, J. M. (2019). Recent progress in modeling imbalance in the atmosphere and ocean. *Phys. Rev. Fluids*, *4*, 010501.
- Takano, Y., Ito, T., & Deutsch, C. (2018). Projected centennial oxygen trends and their attribution to distinct ocean climate forcings. *Global Biogeochem. Cycles*, *32*, 1329–1349. doi: 10.1029/2018GB005939
- Toggweiler, J. R., Russel, J. L., & Carson, S. R. (2006). Midlatitude westerlies, atmospheric CO₂, and climate change during the ice ages. *Paleoceanography*, *21*, PA2005. doi: 10.1029/2005PA001154
- Toggweiler, J. R., & Samuels, B. (1995). Effect of Drake passage on the global thermohaline circulation. *Deep-Sea Res., Part 1, Oceanogr. Res. Pap.*, *42*(4), 477–

500. doi: 10.1016/0967-0637(95)00012-U
- Viebahn, J., & Eden, C. (2012). Standing eddies in the Meridional Overturning Circulation. *J. Phys. Oceanogr.*, *42*, 1496–1508. doi: 10.1175/JPO-D-11-087.1
- Xu, C., Zhai, X., & Shang, X.-D. (2016). Work done by atmospheric winds on mesoscale ocean eddies. *Geophys. Res. Lett.*, *43*, 12174–12180. doi: 10.1002/2016GL071275
- Yang, L., Nikurashin, M., Hogg, A. M., & Sloyan, B. M. (2018). Energy loss from transient eddies due to lee wave generation in the Southern Ocean. *J. Phys. Oceanogr.*, *48*, 2867–2885. doi: 10.1175/JPO-D-18-0077.1
- Zanna, L., Khatiwala, S., Gregory, J. M., Ison, J., & Heimbach, P. (2019). Global reconstruction of historical ocean heat storage and transport. *Proc. Natl. Acad. Sci. USA*, *116*, 1126–1131. doi: 10.1073/pnas.1808838115
- Zhang, Y., & Vallis, G. K. (2013). Ocean heat uptake in eddying and non-eddy ocean circulation models in a warming climate. *J. Phys. Oceanogr.*, *43*, 2211–2229. doi: 10.1175/JPO-D-12-078.1
- Zweng, M. M., Reagan, J. R., Antonov, J. I., Locarnini, R. A., Mishonov, A. V., Boyer, T., . . . Biddle, M. M. (2013). World Ocean Atlas 2013, Volume 2: Salinity. In S. Levitus (Ed.), *Noaa atlas nesdis 74* (pp. 1–39).